

Radiative properties and core-polarization effects in the W^{5+} ion

This article has been downloaded from IOPscience. Please scroll down to see the full text article.

2012 J. Phys. B: At. Mol. Opt. Phys. 45 035002

(<http://iopscience.iop.org/0953-4075/45/3/035002>)

View [the table of contents for this issue](#), or go to the [journal homepage](#) for more

Download details:

IP Address: 193.190.193.1

The article was downloaded on 11/01/2012 at 07:57

Please note that [terms and conditions apply](#).

Radiative properties and core-polarization effects in the W^{5+} ion

S Enzonga Yoca¹, P Palmeri², P Quinet^{2,3}, G Jumet⁴ and É Biémont^{2,3}

¹ Département de Physique, Faculté des Sciences, Université Marien Ngouabi, BP 69 Brazzaville, Congo

² Astrophysique et Spectroscopie, Université de Mons—UMONS, B-7000 Mons, Belgium

³ IPNAS, Université de Liège, B-4000 Liège, Belgium

⁴ Chimie Quantique et Photophysique, Université Libre de Bruxelles, B-1000 Brussels, Belgium

E-mail: enzosat@yahoo.fr

Received 10 November 2011, in final form 12 December 2011

Published 10 January 2012

Online at stacks.iop.org/JPhysB/45/035002

Abstract

The radiative properties of the W^{5+} ion are investigated using two independent theoretical approaches, i.e. the Hartree–Fock method with relativistic corrections of Cowan and the multiconfiguration Dirac–Hartree–Fock method as implemented in the GRASP2K package. The core–valence correlations are studied in detail comparing models where a core-polarization model potential plus a correction to the dipole operator are considered (HFR + CPOL) on the one hand, and core-excited configurations are explicitly included in the configuration–interaction expansion of the atomic state function on the other hand. In general, a good agreement is found between the two theoretical methods. Core-polarization effects are remarkably strong lengthening the lifetimes up to $\sim 15\%$ – 35% and even by a factor of 2 for the 5f levels. The lifetimes of the two 5f levels are found to be model dependent and particularly sensitive to core-penetration effects; precise measurements are clearly needed here.

1. Introduction

Radiative transition probabilities of all the ions of the tungsten isonuclear sequence are needed to model plasmas in fusion reactors. Indeed, the International Thermonuclear Experimental Reactor (ITER) will use tungsten, together with beryllium and carbon-fibre reinforced composites as plasma-facing materials. Tungsten will be sputtered from the plasma wall as a neutral element and will be ionized along its way to the core plasma. The determination of its influx rate to the core plasma will depend on a calculation of transport from the wall surface through the scrape-off layer. Consequently, the identification of emission lines from tungsten ions will greatly aid modelling of the plasma edge and scrape-off layer transport and facilitate the analysis of the net tungsten influx rates.

Recently, the possibility of using extreme ultraviolet emission from low charge states of tungsten ions to diagnose the divertor plasma of ITER tokamak was investigated by Clementson *et al* (2010). To simulate the ITER divertor plasma, tungsten was introduced into the Sustained Spheromak Physics Experiment (SSPX) setup installed at Livermore, while spectral modelling of Lu-like W_{IV} to Gd-like W_{XI} was performed by using the flexible atomic code (FAC). This

study showed that, even if tungsten emission was dominated by W_{VII} , two 5d–5f transitions from W_{VI} were observed at 38.2 and 39.4 nm, but the calculations were not accurate enough to identify other individual lines from this ion.

The data available concerning five-times ionized tungsten (W_{VI}) are rather scarce. In fact, to our knowledge, no radiative parameters have been published so far. Concerning the wavelengths and energy levels, Meijer (1974) was the first to observe the spectrum of W_{VI} obtained from a sliding spark. He identified 13 lines belonging to the 5d 2D –5f $^2F^o$, 5d 2D –6p $^2P^o$, 6s 2S –6p $^2P^o$, 6p $^2P^o$ –6d 2D and 6p $^2P^o$ –7s 2S doublets. This spectrum was later re-measured (Kaufman and Sugar 1976) and extended with the classifications of the 5f $^2F^o$ –5g 2G and 5f $^2F^o$ –6g 2G doublets by Sugar and Kaufman (1979). These latter data were retained in the compilation of Kramida and Shirai (2009).

As a continuous effort to determine the radiative parameters of the lowly charged tungsten ions (W_{I-III}) (Nilsson *et al* 2008, Palmeri *et al* 2008, Quinet *et al* 2010, 2011), this study is dedicated to that matter in order to fill in the gap in W_{VI} . The calculations are described in section 2. The results are discussed in section 3 and conclusions are drawn in section 4.

2. Calculations

Tungsten is the heavy element of the periodic table with $Z = 74$. The ground state of W VI is $5d^2D_{3/2}$ with one valence electron orbiting around a 68 electron-erbium-like ionic core. It is therefore important to consider both the relativistic and the correlation effects in order to correctly describe this atomic structure.

As no measurements are available in the literature, two independent theoretical methods that take into account both effects have been used in this study to calculate and to benchmark the radiative parameters. These are described briefly in the following subsections.

2.1. Hartree–Fock method with relativistic corrections

In the Hartree–Fock method with relativistic corrections (HFR) of Cowan (1981), a set of orbitals is obtained for each electronic configuration by solving the Hartree–Fock equations for the spherically averaged atom. The equations result from the application of the variational principle to the configuration average energy. Relativistic corrections are included in this set of equations, i.e. the Blume–Watson spin–orbit, mass–velocity and one-body Darwin terms. The Blume–Watson spin–orbit term comprises the part of the Breit interaction that can be reduced to a one-body operator.

The multiconfiguration Hamiltonian matrix is constructed and diagonalized in the $LSJM_J\pi$ representation within the framework of the Slater–Condon theory. Each matrix element is a sum of products of Racah angular coefficients and radial integrals (Slater and spin–orbit integrals), i.e.

$$\langle \alpha_a L_a S_a J M_J \pi | H | \alpha_b L_b S_b J M_J \pi \rangle = \sum_i c_i^{a,b} I_i^{a,b}. \quad (1)$$

The radial parameters, $I_i^{a,b}$, can be adjusted to fit the available experimental energy levels in a least-squares approach; $c_i^{a,b}$ are the angular coefficients. The eigenvalues and the eigenstates obtained in this way (*ab initio* or semi-empirically) are used to compute the wavelength and the transition probability for each possible transition.

This technique has been modified (see, e.g., Quinet *et al* (1999)) in order to include the core-polarization effects perturbationally and is referred to as the HFR + CPOL method. In the case of the one-valence-electron system investigated in this work, it consists of adding, to the part of the Hartree–Fock equations related to the valence electron, the following polarization potential (Migdalek and Baylis 1978):

$$V_{\text{CPOL}}(r) = \frac{\alpha_d r^2}{2(r^2 + r_c^2)^3}, \quad (2)$$

where α_d is the static dipole polarizability of the ionic core and r_c its cut-off radius.

There is a corresponding change to the dipole radial matrix element of the length form of the line strength: the integral

$$D_{n\ell, n'\ell'} = \int_0^\infty P_{n\ell}(r) r P_{n'\ell'}(r) dr \quad (3)$$

has to be replaced by

$$D_{n\ell, n'\ell'} = \int_0^\infty P_{n\ell}(r) r \left(1 - \frac{\alpha_d}{(r^2 + r_c^2)^{3/2}} \right) P_{n'\ell'}(r) dr. \quad (4)$$

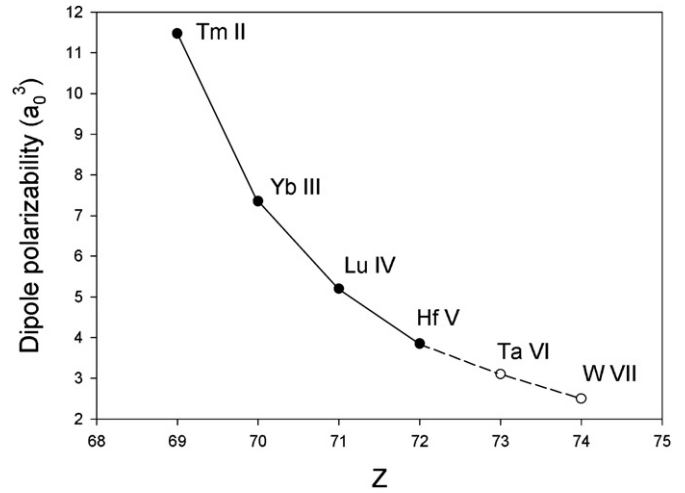


Figure 1. Static dipole polarizability (in a_0^3) along the erbium isoelectronic sequence. Full circles are theoretical values taken from Fraga *et al* (1976). Open circles connected with a dotted line represent extrapolated values.

A further correction, introduced by Hameed and co-workers (Hameed *et al* 1968, Hameed 1972) to allow for a more accurate treatment of the penetration of the core by the valence electron, corresponds to adding to the integral

$$\int_0^\infty P_{n\ell}(r) \frac{r}{(r^2 + r_c^2)^{3/2}} P_{n'\ell'}(r) dr \quad (5)$$

in (4) the core-penetration term

$$\frac{1}{r_c} \int_0^{r_c} P_{n\ell}(r) r P_{n'\ell'}(r) dr. \quad (6)$$

The estimate of the core-polarization contributions requires the knowledge of the dipole polarizability of the ionic core, α_d , and the cut-off radius, r_c . For the first parameter, a value of $\alpha_d = 2.50 a_0^3$ has been graphically extrapolated for W VII from the theoretical values of Fraga *et al* (1976) along the erbium isoelectronic sequence (see figure 1). The cut-off radius, r_c , has been chosen to be equal to $1.20 a_0$ which corresponds to the HFR average value $\langle r \rangle$ for the outermost core orbital (5p).

The configurations retained in the configuration-interaction (CI) expansions were ns ($n = 6 - 7$), nd ($n = 5 - 6$) and ng ($n = 5 - 7$) for the even parity, and np ($n = 6 - 7$) and nf ($n = 5 - 7$) for the odd parity. Although introduced in the calculations, valence–valence correlations are expected to play a minor role here; indeed, it was verified that the 7p, 7d, 6f, 7f and 7g configurations have no effects on the A-values of the transitions between experimentally known energy levels. In addition, the average energies, E_{av} , and the spin–orbit parameters, $\zeta_{n\ell}$, were adjusted with a least-squares optimization procedure minimizing the discrepancies between the calculated and the experimental energy levels compiled by Kramida and Shirai (2009). This calculation is referred to as HFR(A).

In a second calculation referred to as HFR(B), the same model as HFR(A) was used but the core-penetration term (equation (6)) was neglected to show the importance of the latter on the radiative rates.

A third calculation, referred to as HFR(C), was carried out neglecting completely the polarization effects and using the same CI expansion as in HFR(A).

Finally, in order to check the equivalence of the HFR + CPOL method with the explicit inclusion of the interactions with core-excited configurations in the CI expansions, a fourth HFR calculation (HFR(D)) was performed by adding to the above-mentioned CI configuration set the following core-excited configurations: $5s^25p^55d6p$, $5s^25p^55d5f$, $5s5p^65dnd$ ($n = 5-6$), $5s5p^65dns$ ($n = 6-7$) for the even parity, and $5s^25p^55dnd$ ($n = 5-6$), $5s^25p^55dns$ ($n = 6-7$), $5s^25p^55dng$ ($n = 5-6$), $5s5p^65d6p$ and $5s5p^65d5f$ for the odd parity. Further additions of core-excited configurations to the CI expansions were prohibited by our computer limits. Moreover, the $6f$ and 7ℓ ($\ell = p - g$) configurations had to be excluded from the valence configuration list.

2.2. Multiconfiguration Dirac–Hartree–Fock method

In the multiconfiguration Dirac–Hartree–Fock (MCDHF) method implemented in the GRASP2K computer package (Jonsson *et al* 2007), the Hamiltonian is given by

$$H = \sum_{i=1}^N \left(c\alpha_i \cdot \mathbf{p}_i + (\beta_i - 1)c^2 - \frac{Z}{r_i} \right) + \sum_{i<j}^N \frac{1}{r_{ij}}, \quad (7)$$

where c is the speed of light and α and β are the Dirac matrices. The atomic state functions (ASFs) are given as an expansion over jj -coupled configuration state functions (CSFs)

$$|\gamma JM_J \pi\rangle = \sum_i c_i |\alpha_i JM_J \pi\rangle. \quad (8)$$

The CSFs in turn are built from Slater determinants constructed on the four-component Dirac orbitals

$$\phi(r) = \frac{1}{r} \begin{pmatrix} P_{n\kappa}(r) \chi_{\kappa m}(\hat{r}) \\ iQ_{n\kappa}(r) \chi_{-\kappa m}(\hat{r}) \end{pmatrix}. \quad (9)$$

In the above formula, κ is the relativistic angular quantum number, $P_{n\kappa}(r)$ and $Q_{n\kappa}(r)$ are the large and small component radial wavefunctions and $\chi_{\kappa m}(\hat{r})$ is the spinor spherical harmonic in the lsj coupling scheme

$$\chi_{\kappa m}(\hat{r}) = \sum_{m_\ell, m_s} \langle \ell \frac{1}{2} m_\ell m_s | jm \rangle Y_{\ell m_\ell}(\theta, \phi) \xi_{m_s}(\sigma). \quad (10)$$

The radial functions $P_{n\kappa}(r)$ and $Q_{n\kappa}(r)$ are numerically represented on a logarithmic grid and are required to be orthonormal within each κ symmetry. In the MCDHF variational procedure, the radial functions and the expansion coefficients $\{c_i\}$ are optimized to self-consistency.

The relativistic two-body Breit interaction and the quantum electrodynamic corrections due to self-energy and vacuum polarization are also considered through the implementation of the routines developed by McKenzie *et al* (1980).

The calculations have been focused on the first 11 experimental levels of W VI belonging to the configurations $5d$, $5f$, $6s$, $6p$ and $6d$ with $J = 1/2-7/2$ (Kramida and Shirai 2009). A Fermi charge distribution has been used for the nucleus with $Z = 74$. The orbitals have been optimized in three steps. In the first step, the core orbitals, i.e. $1s$ to $5p$,

Table 1. Comparison of *ab initio* MCDHF-EOL and RCI level energies (E) and fine-structure splittings (FS) with experimental values in W VI.

Level ^a	E_{exp}^a (cm^{-1})	FS_{exp}^a (cm^{-1})	E_{DHF}^b (cm^{-1})	FS_{DHF}^b (cm^{-1})	E_{RCI}^c (cm^{-1})	FS_{RCI}^c (cm^{-1})
$5d \ ^2D_{3/2}$	0.0	8709.3	0	8008	0	8309
$5d \ ^2D_{5/2}$	8709.3		8008		8309	
$6s \ ^2S_{1/2}$	79 431.3		80 407		77 212	
$6p \ ^2P_{1/2}^o$	147 553.1	17 483.6	147 409	16 415	143 971	16 885
$6p \ ^2P_{3/2}^o$	165 036.7		163 824		160 855	
$5f \ ^2F_{5/2}^o$	261 681	749	263 236	204	258 412	651
$5f \ ^2F_{7/2}^o$	262 430		263 440		259 063	
$6d \ ^2D_{3/2}$	261 694.6	2717.1	258 187	2613	257 301	2663
$6d \ ^2D_{5/2}$	264 411.7		260 800		259 964	

^a Kramida and Shirai (2009).

^b MCDHF-EOL calculation.

^c RCI calculation.

together with the $5d$ orbital, have been optimized. The two CSFs of the ground configuration $5d$ were retained in the configuration space. The energy functional was built within the framework of the average level (AL) option (Grant 1988). The second step consisted in increasing the configuration space by considering all of the four CSFs belonging to the $5d$ and $5f$ configurations. The $5f$ orbital has been optimized, keeping the others fixed to their values of the first step. The AL option was chosen to build the energy functional. In the final optimization step, the configuration space has been extended to the 13 CSFs belonging to the configurations $5d$, $5f$, $6s$, $6p$, $6d$ and $6f$. Only the $n = 6$ orbitals have been optimized, fixing all the others to the values of the preceding step using an energy functional built on the lowest 11 ASFs within the framework of the extended optimal level (EOL) option (Grant 1988). In this final step, to be referred to as the MCDHF-EOL calculation, only the valence correlations have been taken into account. Core–valence correlations were finally included by extending further the configuration space as follows: single and double virtual electron excitations to an active orbital set $\{5s, 5p, 5d, 5f, 6s, 6p, 6d, 6f\}$ from the multireference configurations $5s^25p^65d + 5s^25p^65f + 5s^25p^66p$ have been considered with fixed total angular momenta $J = 1/2-7/2$. A relativistic configuration-interaction (RCI) calculation (Grant 1988) has been then carried out using the preceding MCDHF-EOL orbitals and diagonalizing a Hamiltonian matrix built with the 35 434 CSFs generated. A comparison of the level energies and the fine-structure splittings (FS) is presented in table 1 in order to give an idea of the quality of both *ab initio* fully relativistic calculations. Although the RCI level energies are systematically a few thousand cm^{-1} lower than experiment, the RCI FS values are improved with respect to the MCDHF-EOL ones. In the calculation of the transition rates, the theoretical transition energies have been replaced by the experimental values taken from the compilation of Kramida and Shirai (2009) for both the MCDHF-EOL and RCI calculations. These empirical corrections increased the rates by $\sim 1\%$ – 8% for the E1 transitions and by $\sim 15\%$ – 30% for the forbidden lines.

Table 2. Comparison of calculated lifetimes in W VI.

Level ^a	$E^a(\text{cm}^{-1})$	Lifetime (s) ^b					
		RCI ^c	MCDHF-EOL ^d	HFR(A) ^e	HFR(B) ^f	HFR(C) ^g	HFR(D) ^h
5d $^2D_{5/2}$	8 709.3	1.40(−1)/1.40(−1)	1.40(−1)/1.40(−1)	1.40(−1)	1.40(−1)	1.40(−1)	1.40(−1)
6s $^2S_{1/2}$	79 431.3	3.60(−4)/4.18(−4)	3.66(−4)/4.37(−4)	3.77(−4)	3.68(−4)	3.68(−4)	3.65(−4)
6p $^2P_{1/2}^o$	147 553.1	1.71(−10)/1.79(−10)	1.46(−10)/1.67(−10)	1.86(−10)	1.89(−10)	1.56(−10)	1.84(−10)
6p $^2P_{3/2}^o$	165 036.7	1.34(−10)/1.40(−10)	1.20(−10)/1.34(−10)	1.39(−10)	1.40(−10)	1.14(−10)	1.36(−10)
5f $^2F_{5/2}^o$	261 681	5.47(−11)/5.74(−11)	3.22(−11)/3.61(−11)	6.50(−11)	4.80(−11)	3.14(−11)	6.55(−11)
6d $^2D_{3/2}$	261 694.6	1.65(−10)/1.72(−10)	1.43(−10)/1.50(−10)	1.58(−10)	1.56(−10)	1.33(−10)	1.54(−10)
5f $^2F_{7/2}^o$	262 430	5.21(−11)/5.46(−11)	3.31(−11)/3.73(−11)	7.10(−11)	5.25(−11)	3.43(−11)	6.45(−11)
6d $^2D_{5/2}$	264 411.7	2.02(−10)/2.11(−10)	1.77(−10)/1.87(−10)	2.24(−10)	2.21(−10)	1.88(−10)	2.18(−10)
7s $^2S_{1/2}$	278 915.5			1.40(−10)	1.44(−10)	1.48(−10)	1.40(−10)
5g $^2G_{9/2}$	362 222			1.64(−10)	1.61(−10)	1.41(−10)	1.61(−10)
5g $^2G_{7/2}$	362 234			1.61(−10)	1.59(−10)	1.39(−10)	1.58(−10)

^a Kramida and Shirai (2009).^b $A(B)$ stands for $A \times 10^B$.^c RCI calculation up to 6f including 5s and 5p core-excited configurations. A/B stands for Babushkin/Coulomb gauge values. Values are corrected from the experimental transition energies.^d MCDHF-EOL calculation up to 6f. A/B stands for Babushkin/Coulomb gauge values. Values are corrected from the experimental transition energies.^e HFR + CPOL calculation up to 7g.^f HFR + CPOL calculation up to 7g excluding penetration.^g HFR calculation up to 7g.^h HFR calculation up to 6g including 5s and 5p core-excited configurations.

3. Results and discussion

In table 2, the radiative lifetimes of the experimental levels of W VI (Kramida and Shirai 2009) calculated using different MCDHF and HFR models are compared. The 6g levels had to be excluded from that table because the E1 decay transitions to the 6f levels contribute significantly to the 6g lifetime but the 6f energies are not known experimentally. Differences between RCI and MCDHF-EOL sets show the core–valence correlation effects, i.e. the core-polarization effects, on the lifetimes in the context of the MCDHF method, whereas, in the HFR method, this is done by comparing HFR(A), HFR(B) or HFR(D) with HFR(C). Core-penetration effects are displayed by comparing HFR(B) with HFR(A). Comparing HFR(D) with HFR(A) shows the equivalence between the use of a core-polarization model potential and the explicit consideration of core-excited configurations in the CI expansion. Although it is a necessary but not sufficient condition, the quality of both MCDHF calculations (RCI and MCDHF-EOL) can also be appreciated by the good agreement between the gauges. Unfortunately, HFR does not allow for the calculation of the transition probabilities in the velocity gauge.

With the exceptions of the level $7s^2S_{1/2}$ and the two metastable levels $5d^2D_{5/2}$ and $6s^2S_{1/2}$, the core-polarization effects tend to systematically lengthen the lifetimes up to $\sim 15\%$ – 35% and even by a factor of 2 for the 5f levels. The HFR(D) calculations reproduced remarkably well the HFR(A) lifetimes demonstrating the equivalence of both treatments of the core–valence correlations. Generally, both MCDHF calculations (RCI and MCDHF-EOL) support their HFR counterparts (respectively: HFR(A), HFR(D) and HFR(C)) except for both 5f levels for which the polarization effects seem to be underestimated by our RCI model. Concerning the latter ones, the HFR(B) lifetimes indicate a higher sensitivity to core

Table 3. Comparison of dipole radial integrals in W VI.

Dipole	$D_{nl,n'l'}(\text{au})$		
	HFR(A) ^a	HFR(B) ^b	HFR(C) ^c
5d–6p	1.43	1.42	1.54
5d–5f	1.73	2.01	2.49
6s–6p	2.08	2.11	2.42
6d–6p	−3.35	−3.37	−3.66
6d–5f	−4.44	−4.35	−4.59

^a HFR + CPOL calculation.^b HFR + CPOL calculation excluding penetration.^c HFR calculation where the core-polarization effects are neglected.

penetration in comparison to the other atomic states. In this respect, the dipole radial integrals, $D_{nl,n'l'}$, for different parity-changing single-electron jumps, are compared for HFR(A), HFR(B) and HFR(C) calculations in table 3. One can note the strong decrease of the $D_{5d,5f}$ integral due to core penetration with respect to all of the others. Moreover, figure 2 displays the strong penetration into the core-electron density probabilities of the 5d and 5f valence orbitals. These can therefore explain the important variation of the 5f lifetimes due to core penetration keeping in mind that these lifetimes are dominated by the 5d–5f decay channels. With respect to this, the disagreements between, on the one hand, HFR(A) and HFR(D) and, on the other hand, RCI indicate a model dependency probably due to slight differences in the overlaps between core and valence orbitals; therefore, precise lifetime measurements are clearly needed here.

In figure 3, the E1 transition probabilities calculated with our best MCDHF (RCI) and HFR (HFR(A)) models are compared. For RCI, the Babushkin gauge values which correspond, at the non-relativistic limit, to the length form

Table 4. Decay channels of the metastable states in W VI: comparison of the HFR(A) and RCI A-values.

			A_{ki} (s^{-1})		
Decay channel	Type		HFR(A) ^a	RCI ^b	
5d ² D _{5/2}	–	5d ² D _{3/2}	M1	7.16(0)	7.12(0)
		5d ² D _{3/2}	E2	2.58(–3)	2.54(–3)
6s ² S _{1/2}	–	5d ² D _{3/2}	E2	1.44(3)	1.45(3)
		5d ² D _{5/2}	E2	1.21(3)	1.33(3)

^a HFR+CPOL calculation. $A(B)$ stands for $A \times 10^B$.

^b RCI calculation. $A(B)$ stands for $A \times 10^B$. E2 A-values are shown in the Babushkin gauge. Values are corrected from the experimental transition energies.

used in HFR calculations are plotted. The agreement between both sets is good (~10%–15%) except for, again, the 5d–5f transitions (the two largest rates appearing in this figure) for which the disagreements grow up to ~30%–35% due to the sensitivity of the $D_{5d,5f}$ dipole transition radial integral to the core-penetration effects. Without the empirical corrections in RCI, the agreement between both models would be slightly better with ~25%–30% for the 5d–5f transitions and ~5%–15% for the others.

Table 4 presents a comparison of M1/E2 transition probabilities calculated using our HFR(A) and RCI models (in the Babushkin gauge for the E2 transitions). Excellent agreement is found between both calculations ($\leq 10\%$). One can see that the decay of the 5d ²D_{5/2} metastable state is dominated by the M1 channel. Unlike the E1 transitions, the

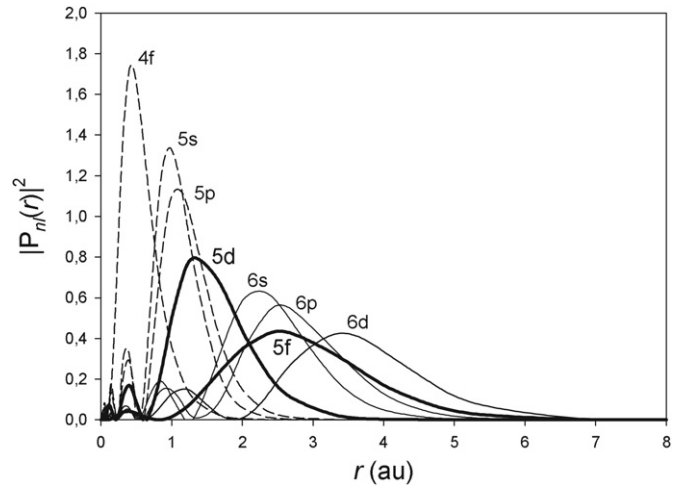


Figure 2. HFR orbital density probabilities. The core orbitals (limited down to 4f) are represented with dashed lines and the valence orbitals with continuous lines (the 5d and 5f orbitals are in bold). The importance of the penetration of the valence orbitals into the ionic core can be seen.

empirical corrections in RCI brought significant improvements in the agreement between both models; without it, the disagreement would grow up to ~30%.

Finally, the weighted oscillator strengths (in a logarithmic scale) and transition probabilities, as calculated with our best HFR(A) model, are given in table 5 for all the important E1, M1 and E2 transitions connecting the experimental levels of W VI published by Sugar and Kaufman (1979) retained in the

Table 5. Oscillator strengths ($\log gf_{ik}$) and transition probabilities (gA_{ki}) for important transitions in W VI.

λ^a (nm)	Lower level ^a		Upper level ^a		Type	$\log gf_{ik}^c$	gA_{ki}^c (s^{-1})
	E (cm^{-1})	Designation	E (cm^{-1})	Designation			
38.2145	0.0	5d ² D _{3/2}	261 681	5f ² F _{5/2} ^o	E1	0.28	8.68(10)
39.4133	8709.3	5d ² D _{5/2}	262 430	5f ² F _{7/2} ^o	E1	0.42	1.13(11)
39.5301	8709.3	5d ² D _{5/2}	261 681	5f ² F _{5/2} ^o	E1	–0.88	5.60(9)
60.5929	0.0	5d ² D _{3/2}	165 036.7	6p ² P _{3/2} ^o	E1	–0.86	2.49(9)
63.9687	8709.3	5d ² D _{5/2}	165 036.7	6p ² P _{3/2} ^o	E1	0.07	1.91(10)
66.9315	261 681	5f ² F _{5/2} ^o	411 087	6g ² G _{7/2}	E1	–0.07	1.28(10)
67.2726	262 430	5f ² F _{7/2} ^o	411 079	6g ² G _{9/2}	E1	0.05	1.64(10)
67.7718	0.0	5d ² D _{3/2}	147 553.1	6p ² P _{1/2} ^o	E1	–0.21	8.91(9)
76.1252	147 553.1	6p ² P _{1/2} ^o	278 915.5	7s ² S _{1/2}	E1	–0.27	6.21(9)
87.6106	147 553.1	6p ² P _{1/2} ^o	261 694.6	6d ² D _{3/2}	E1	0.41	2.25(10)
87.8128	165 036.7	6p ² P _{3/2} ^o	278 915.5	7s ² S _{1/2}	E1	–0.03	8.09(9)
99.4502	261 681	5f ² F _{5/2} ^o	362 234	5g ² G _{7/2}	E1	0.85	4.78(10)
100.1964 ^b	262 430	5f ² F _{7/2} ^o	362 234	5g ² G _{7/2}	E1	–0.58	1.75(9)
100.2085	262 430	5f ² F _{7/2} ^o	362 222	5g ² G _{9/2}	E1	0.96	6.11(10)
100.6289	165 036.7	6p ² P _{3/2} ^o	264 411.7	6d ² D _{5/2}	E1	0.61	2.68(10)
103.4575	165 036.7	6p ² P _{3/2} ^o	261 694.6	6d ² D _{3/2}	E1	–0.36	2.74(9)
116.8151	79 431.3	6s ² S _{1/2}	165 036.7	6p ² P _{3/2} ^o	E1	0.18	7.32(9)
125.8950 ^b	0.0	5d ² D _{3/2}	79 431.3	6s ² S _{1/2}	E2	–6.16	2.88(3)
141.3987 ^b	8709.3	5d ² D _{5/2}	79 431.3	6s ² S _{1/2}	E2	–6.14	2.42(3)
146.7958	79 431.3	6s ² S _{1/2}	147 553.1	6p ² P _{1/2} ^o	E1	–0.23	1.85(9)
1147.8836 ^b	0.0	5d ² D _{3/2}	8709.3	5d ² D _{5/2}	M1	–6.07	4.30(1)
1147.8836 ^b	0.0	5d ² D _{3/2}	8709.3	5d ² D _{5/2}	E2	–9.51	1.55(–2)

^a From Sugar and Kaufman (1979).

^b Wavelengths deduced from the experimental levels and are given in air for those greater than 200 nm.

^c HFR(A) (this work). $A(B)$ stands for $A \times 10^B$.

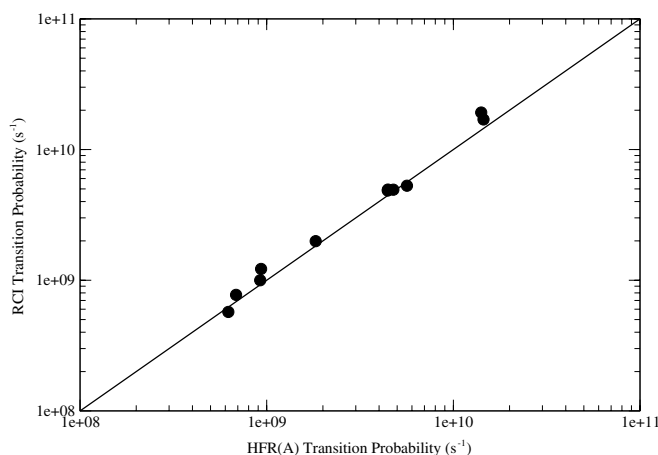


Figure 3. Comparison of the E1 transition probabilities between the RCI (in the Babushkin gauge) and HFR(A) calculations. RCI values are corrected from the experimental transition energies. A straight line of equality has been drawn.

compilation of Kramida and Shirai (2009). These radiative parameters should be of interest in fusion research.

4. Conclusions

The radiative properties of W_{VI} have been studied using two independent theoretical methods, i.e. the HFR and the fully relativistic MCDHF methods. In particular, the core-polarization effects on the transition probabilities have been investigated in detail considering, on the one hand, a core-polarization model potential plus a correction to the dipole operator and, on the other hand, the direct inclusion of core-excited configurations in the CI expansion.

Both approaches of the core-valence correlations are found to be equivalent and these interactions tend in general to lengthen systematically the radiative lifetimes up to $\sim 15\%$ – 35% and even by a factor of 2 for the 5f levels. Both independent methods agree to each other within $\sim 10\%$ – 15% except for the 5d–5f E1 transitions (where disagreements reach up to $\sim 30\%$ – 35%) which are notably sensitive to the core-penetration effects. Here, precise measurements of the lifetimes of the 5f levels are clearly in need.

Acknowledgments

This work was supported by the Belgian FNRS and the ADAS-EU project. SEY would like to thank this organization for funding his stay in Belgium (grant 2011/V 6/5/013-IB/JN-1343) and his colleagues from Université de Mons—UMONS for their kind hospitality. He would also like to acknowledge the support from Université Marien Ngouabi. EB, PQ and PP are respectively Research Director, Senior Research Associate and Research Associate of the FNRS.

References

- Clementson J, Beiersdorfer P, Magee E W, McLean H S and Wood R D 2010 *J. Phys. B: At. Mol. Opt. Phys.* **43** 144009
- Cowan R D 1981 *The Theory of Atomic Structure and Spectra* (Berkeley, CA: University of California Press)
- Fraga S, Karwowski J and Saxena K M S 1976 *Handbook of Atomic Data* (Amsterdam: Elsevier)
- Grant I P 1988 *Method of Computation Chemistry* vol 2, ed S Wilson (New York: Plenum) p 1
- Hameed S 1972 *J. Phys. B: At. Mol. Phys.* **5** 746
- Hameed S, Herzenberg A and James M G 1968 *J. Phys. B: At. Mol. Phys.* **1** 822
- Jonsson P, He X, Froese Fischer C and Grant I P 2007 *Comput. Phys. Commun.* **177** 597
- Kaufman V and Sugar J 1976 *J. Opt. Soc. Am.* **66** 1019
- Kramida A E and Shirai T 2009 *At. Data Nucl. Data Tables* **95** 305
- McKenzie B J, Grant I P and Norrington P H 1980 *Comput. Phys. Commun.* **21** 233
- Meijer F G 1974 *Physica* **73** 415
- Migdalek J and Baylis W E 1978 *J. Phys. B: At. Mol. Phys.* **11** L497
- Nilsson H, Engström L, Lundberg H, Palmeri P, Fivet V, Quinet P and Biémont É 2008 *Eur. Phys. J. D* **49** 13
- Palmeri P, Quinet P, Fivet V, Biémont É, Nilsson H, Engström L and Lundberg H 2008 *Phys. Scr.* **78** 015304
- Quinet P, Palmeri P and Biémont É 2011 *J. Phys. B: At. Mol. Opt. Phys.* **44** 145005
- Quinet P, Palmeri P, Biémont É, McCurdy M M, Rieger G, Pinnington E H, Wickliffe M E and Lawler J E 1999 *Mon. Not. R. Astron. Soc.* **307** 934
- Quinet P, Vinogradoff V, Palmeri P and Biémont É 2010 *J. Phys. B: At. Mol. Opt. Phys.* **43** 144003
- Sugar J and Kaufman V 1979 *J. Opt. Soc. Am.* **69** 141